N75 19159

A DIRECT PROCEDURE FOR PARTITIONING SCANNING WORKLOAD IN CONTROL DISPLAY SYSTEM DESIGN*

W. F. Clement, L. G. Hofmann, and D. Graham

Systems Technology, Inc.
Princeton, New Jersey

ABSTRACT

Recent experimental eye scanning measurements from simulated instrument approaches in a flight-like cockpit representing a contemporary jet transport have made it possible to simplify the procedure for predicting the partition of the pilot's scanning workload required for monitoring and controlling a task with status displays and a flight director. When there is but a single director control display, the new procedure eliminates iteration in the preliminary design computations. The preliminary design computations are based on predictions of closed-loop input-correlated errors in displayed variables with respect to the trimmed flight values. Also included are methods for predicting multiloop error coherence and for correcting the predicted partition of scanning workload when the pilot's scanning remnant contribution is significant.

*This research was sponsored by the U.S. Air Force Flight Dynamics Laboratory under Contract No. F33615-71-C-1349.

INTRODUCTION

Scanning of an instrument panel permits the displayed information to be sampled foveally. The foveal fixation dwell time interval is variable, but averages about one-half second. Information outside the foveal region may perhaps be observed parafoveally. One can measure the transition of foveal fixation between two instruments and the pause or dwell of the visual axis of fixation on an informative part of the instrument (for example the tip of a pointer) before beginning the next transition. Measurements have shown variability in the time interval which elapses between successive fixations on the same instrument. This time interval is called the scan interval or sampling interval. It will in general exhibit a different ensemble average value for each point of fixation. Besides instrument-to-instrument scans, scanning may occur among the elements of combined displays.

The pilot using a flight director for control wants to spend a certain amount of time monitoring the confidence-inspiring situation information. This is how he gains and maintains confidence in the flight director. We speak of this time that he spends monitoring the situation information as his monitoring workload margin. It can be expressed either as a fraction of time, the dwell fraction, or as the fraction of the number of looks, the look fraction. Sufficient monitoring margin is essential to the pilot. This need for monitoring margin can lead to a possible conflict with the addition of a third director command for direct lift control or thrust control which requires a separate foveal fixation. Unless the flight director presentation can be contrived to convey three director commands in one fixation through foveal and parafoveal channels of awareness, the switching of attention between the two-command flight director and a third director command may produce considerably more remnant in all three director commands.

In order that we may more clearly appreciate these effects, one purpose in this investigation has been to improve the models for predicting the partition of the pilot's time and the number of fixations between the monitoring

margin and the fraction of time required for control using the director commands. We shall begin here with a review of key experimental results from Ref. 1, supported by a companion paper, Ref. 2, in order to introduce a new, simpler, direct method for partitioning scanning workload with a flight director. We will then show how the properties of the pilot's scanning remnant and properties of the partition of scanning workload may conspire to compromise the pilot's confidence in his situation, to compromise his performance, or both, so that his subjective impression of the overall task workload will be high. The presentation has been subdivided for convenience into the following topics, the last of which is a summary.

- Review of Eye Scanning Data
- Summary of the Revised Model for Partitioning Scanning Workload
- A Simplified Partitioning Procedure for a Single Director Control Display
- A Cause of Low Error Coherence
- Estimation of Error Coherence and Variance
- Modification of the Input-Correlated Predictions of Average Threshold Exceedence Frequency
- Summary of the Simplified Direct Procedure for Partitioning Scanning Workload with a Flight Director

REVIEW OF EYE SCANNING DATA

A Model for Display Monitoring

In order to maintain confidence in a flight director for closed-loop tracking, the pilot must also attend to the open-loop monitoring of situation or status displays to perceive exceedence of tolerances or specified values related to the task. Most of the pilot's status displays present the flight motion variables which are constituents of the flight director commands. Other status displays are common to engine or radar instrument monitoring, where effects of manual control are not displayed.

We shall include time for monitoring the status displays appropriate to the flight director loops and the relatively open-loop displays such as engine, fuel management, navigation, and communication displays by estimating an average dwell interval of 0.4 sec (Ref. 3) and a scanning frequency equal to an appropriate threshold exceedence frequency for the display. The average threshold exceedence frequency, $\bar{f}_{|x_i|}$, (Ref. 4) for Gaussian random signals is

$$\bar{f}_{|x_i|} = \frac{a}{\pi} e^{-x_i^2/2\sigma_x^2} \left(\frac{\sigma_{\dot{x}}}{\sigma_x}\right)$$

where x_i is the threshold of exceedence, σ_x^2 is the variance of the displayed signal, and $\sigma_{\dot{x}}^2$, the variance of the rate of change of the displayed signal. The resulting fractional scanning workload for monitoring (that is, the product of 0.4 sec with the sum of the scanning frequencies for the monitored displays) is then compared with that for the tracking control tasks to determine whether or not both tracking control and monitoring tasks can be performed within the available time constraint. This comparison and determination is called the "partition" of scanning workload for monitoring and control.

Each average monitored display scanning frequency, $\bar{f}_{s_i}$, ies, is assumed to be equal to the expected frequency, $\bar{f}_{|x_i|}$, with which a certain level, $|x_i|$, of the displayed variable, x, is exceeded

$$\bar{f}_{s_i} = \frac{a}{\pi} e^{-\frac{K^2}{2}} \left(\frac{\sigma_{\dot{x}}}{\sigma_x}\right)_i \qquad (1)$$

where K is the ratio of an exceedence threshold level, $|x_i|$, to σ_x

σ_x is the standard deviation of the displayed signal

$\sigma_{\dot{x}}$ is the standard deviation of the time rate of change of the displayed signal

i is an index which denotes the particular display

S denotes the set of monitored displays

We have expressed the level of exceedence in terms of $K\sigma_x$ in Eq. 1. We have determined that K ranges from 1.4 to 3.0 for the data in Ref. 1 with a value of 2.0 being representative overall. Presumably the lower the value of K the lower the pilot's threshold of indifference to the displayed situation which he is monitoring, and the greater his confidence in the task performance.

Results of Dwell Fraction Analysis

Using the subject-averaged scanning statistics of Ref. 1, a correlation of scanning workload (dwell fraction) and flight director system bandwidth (i.e., crossover frequency) has been made. This correlation in Ref. 1 shows that the higher the crossover frequency the higher the dwell fraction and the lower the corresponding scanning rate on the flight director. The conclusion is that the most efficient scanning policy is to fixate as infrequently as possible. This minimizes the 0.2 sec latency effect associated with each fixation required for monitoring or control. In other words, the instrument monitoring requirements place a lower bound on the flight director scanning rate. Since the sum of the flight director and monitoring foveal dwell fractions cannot exceed unity (less an allowance, M_s, for saccades and blinks), we can write Eq. 2 for the partition of dwell fraction between director displays and monitored displays.

$$\sum_{j \in P} \eta_j = 1 - M_s - 0.4 \sum_{i \in S} \bar{f}_{e_i} \qquad (2)$$

In Eq. 2, P is the set of (primary) director command displays and S is the set of (secondary) monitored displays. Other symbols are defined in Table I.

Results of Look Fraction Analysis

Reference 2 has further examined the eye-movement data summarized in Ref. 1. This was for the purpose of discerning the effects of the number of primary displays and the degree of display integration upon scanning behavior. Scans among secondary (monitored) instruments were found to be exceedingly rare, and scans which begin and end at the same instrument were also found to be rare. Examination of the eye movement data for evidence of

TABLE I

Definitions of Symbols

adj [ ]	the adjoint operator, i.e., the transposed matrix of cofactors of [ ]
e	Naperian base, 2.71828...
$\bar{f}_s$	average scanning frequency ($1/\bar{T}_s$) (Hz)
$\bar{f}_{\lvert x_i \rvert}$	average threshold exceedence frequency for the absolute threshold x_i (Hz)
$i \in P$	index i ranges over the set P
i, j, k	indices designating instruments or points of fixation
n_{e_j}	the pilot's remnant injected at the j^{th} axis of the flight director
P	number of primary control displays, instruments, or points of fixation
q_{ij}	link value or probability of fixation transition from i to j
x_i	threshold of exceedence for a displayed variable x
ADI	attitude director indicator
F	foveal
FD	flight director
K	$\lvert x_i \rvert / \sigma_x$
M_s	dwell fraction margin for saccades and blinks
N	total number of fixations or "looks" in a time interval
P	set of primary (director control) displays or instruments
S	set of secondary (monitored) displays or instruments
$\bar{T}_d$	average foveal dwell interval ($\eta \bar{T}_s$) (sec)
$\bar{T}_{d_e}$	average effective dwell interval ($\eta_e \bar{T}_s$) (sec)
T_R	an arbitrary time interval (sec)
$\bar{T}_s$	average scanning interval ($1/\bar{f}_s$) (sec)

P-134

TABLE I (cont'd)

Definitions of Symbols

δ_{ij}	Kronecker delta
ϵ	error with respect to the trimmed value of a displayed variable
ϵ_i	input-correlated error
η	average foveal dwell fraction ($\bar{T}_d / \bar{T}_s = \bar{f}_s \bar{T}_d$)
η_e	average effective dwell fraction ($\bar{T}_{d_e} / \bar{T}_s = \bar{f}_s \bar{T}_{d_e}$)
ι_κ	independent external input or forcing function acting on the director control system
ν_i	average look fraction, $\lim_{N\to\infty} N_i / N = (\bar{f}_{s_i} / \bar{f}_s)$
π	3.14159...
$\sigma^2_{o_x}$	input-correlated variance of x
$\sigma^2_{o_{\dot{x}}}$	input-correlated variance of dx/dt
$\sigma^2_{i_x}$	uncorrelated variance of x
$\sigma^2_{i_{\dot{x}}}$	uncorrelated variance of dx/dt
σ^2_x	variance of x
$\sigma^2_{\dot{x}}$	variance of dx/dt
$\lvert\Delta_s\rvert$	coherence determinant
Σ	summation operator
$\Phi_{nn_s}(\omega)$	power spectral density of sampling (or scanning) remnant (units/rad/sec)
Ω	parafoveal-to-foveal gain ratio

scans within an instrument face also has shown that such scans are rare. This being the case, the scanning workload imposed by the need for monitoring* will be reduced by the degree of integration of the information for monitoring within the primary displays. This is because it is an observed fact that when integrated in this manner, information for monitoring does not contribute to the scanning workload.

Viewed in another way, the monitoring workload will increase as the frequency of scans to secondary instruments increases. This is because the average dwell time, $\bar{T}_{d_i}$, for each separate monitoring fixation is 0.4 sec with little variability. The sum of the average scanning frequencies for the separated secondary instruments is the average frequency of scans for monitoring, $\sum_{i\in S} \bar{f}_{s_i}$, where the summation is over the set, S, of secondary instruments.

The average fraction of scans employed for monitoring is called the monitoring look fraction, $\sum_{i\in S} \nu_i = \sum_{i\in S} \bar{f}_{s_i} / \bar{f}_s$ where $\bar{f}_s$ is the overall average scanning frequency defined for the total number, N, of primary and secondary looks (i.e., fixations) in an interval of time T_R by $\bar{f}_s = \lim_{N\to\infty} (N / T_R)$. Since the sum of the primary and secondary look fractions cannot exceed unity, we can write Eq. 3 for the partition of look fraction between primary displays and monitored displays.

$$\sum_{j\in P} \nu_j = 1 - \left(\sum_{i\in S} \bar{f}_{s_i} / \bar{f}_s\right) \qquad (3)$$

where ν_j is the look fraction for each primary display.

*It should be noted that pilots refer to the instrument monitoring function as "cross-checking."

SUMMARY OF THE REVISED MODEL FOR PARTITIONING SCANNING WORKLOAD

The results of the dwell and look fraction analyses can be used in combination to simplify considerably the display theory computations for the single command display case. The simplification is such that iterative computations which are ordinarily required are replaced by direct computation of the average scanning frequencies for the flight director and secondary instruments. As a result, the scanning workload margin required for monitoring given previously $0.4 \sum_{i \in S} \bar{f}_{s_i}$, is easily evaluated.

Equations 1, 2, and 3, introduced previously, provide the basis for the partition of scanning workload for monitoring and control. The results of the partition provide estimates of the average scanning frequencies and dwell fractions for control as well as monitoring. The dwell fractions also represent the temporal probabilities of fixation, whereas the look fractions represent the ensemble probabilities of fixation. From these predictions, one can estimate the dwell intervals, look intervals, link values, and other scanning parameters desired. A revised model for the prediction of link values in a flight director is given in a companion paper, Ref. 2.

The detailed development of a simplified approximate method for partitioning the scanning workload required for monitoring and control in a task with a single primary director display is given in the next topic. The simplified approximate method will be increasingly more accurate as the pilot's tracking error coherence approaches unity. Following the presentation of the simplified method we shall show how to test for multiloop error coherence, and how to correct the partition of scanning workload in case of low error coherence caused by the pilot's injection of scanning remnant.

A SIMPLIFIED PARTITIONING PROCEDURE FOR A SINGLE DIRECTOR CONTROL DISPLAY

By way of convenience in what follows, we shall define the director control display as "primary" and the situation displays for monitoring as "secondary."

A special case of the revised pilot model for scanning described in Ref. 2 applies when a single director control display is used. In this case, the average scanning frequency for the flight director, $\bar{f}_{s_{FD}}$, is equal to the sum of the average scanning frequencies for the secondary displays. That is

$$\bar{f}_{s_{FD}} = \sum_{i \in S} \bar{f}_{s_i} \tag{4}$$

where S is the set of secondary displays and the $\bar{f}_{s_i}$ are given by Eq. 1. By virtue of the fundamental requirement that all of the pilot's fixations be accounted for, Eq. 4 is also equal to $\bar{f}_s / 2$, where $\bar{f}_s$ is the average scanning frequency.

The event of this simple relationship suggests the following basis for the prediction of the scanning workload margin required for monitoring the situation. Equation 4 may be interpreted as giving the frequency with which fixation of the primary display is <u>interrupted</u> in terms of the individual situation display monitoring scanning frequencies. If we add to this the assumption that the pilot scans for the purpose of monitoring only as frequently as is required to maintain a personal confidence level in the <u>situation</u>, we have sufficient conditions for the existence of an optimum monitoring policy.

A partition of scanning workload (or dwell fraction) between the flight director and the set of secondary displays leads to Eq. 5. Equation 5 is for the foveal dwell fraction on the flight director under the assumption that the dwells for saccades and blinks are negligible ($M_s = 0$). It is a special case of Eq. 2.

$$\eta_{FD} = 1 - 0.4 \sum_{i \in S} \bar{f}_{s_i} \tag{5}$$

Equation 5 indeed shows that monitoring is accomplished at the expense of the flight director dwell fraction. Thus, the dwell fraction on the flight director becomes, by virtue of Eqs. 4 and 5:

$$\eta_{FD} = 1 - 0.4\,\bar{f}_{s_{FD}} \tag{6}$$

The effective dwell fraction on the flight director is defined (Ref. 6) by

$$\eta_{e_{FD}} \triangleq \eta_{FD} + \Omega_{FD}(1 - \eta_{FD}) \tag{7}$$

where Ω_{FD} is the parafoveal-to-foveal gain ratio. The effective dwell fraction on the flight director will be greater than or equal to the actual dwell fraction as Ω_{FD} is varied from 1.0 to 0. An alternate expression for Eq. 7 is obtained upon substitution of Eq. 6.

$$\eta_{e_{FD}} = 1 - 0.4\,\bar{f}_{e_{FD}}(1 - \Omega_{FD}) \tag{8}$$

The complement of the effective dwell fraction is the effective interrupt fraction. This is obtained by rearranging Eq. 8.

$$1 - \eta_{e_{FD}} = 0.4\,\bar{f}_{e_{FD}}(1 - \Omega_{FD}) \tag{8a}$$

The flight director average scanning interval is the reciprocal of the average scanning frequency, $\bar{T}_{s_{FD}} = 1/\bar{f}_{s_{FD}}$.

The average foveal dwell interval on the flight director can be obtained by multiplying Eq. 6 through by $\bar{T}_{s_{FD}}$ and using the definition (Ref. 3) of dwell fraction, $\eta_{FD} \triangleq \bar{T}_{d_{FD}}/\bar{T}_{s_{FD}}$.

$$\bar{T}_{d_{FD}} = \bar{T}_{s_{FD}} - 0.4 \tag{9}$$

The effective dwell interval on the flight director is greater than the foveal dwell interval if parafoveal perception is not inhibited. The effective dwell interval can be obtained by multiplying Eq. 8 by $\bar{T}_{s_{FD}}$ since $\bar{T}_{d_{e_{FD}}} = \eta_{e_{FD}}\,\bar{T}_{s_{FD}}$.

$$\bar{T}_{d_{e_{FD}}} = \bar{T}_{s_{FD}} - 0.4(1 - \Omega_{FD}) \tag{10}$$

Equation 9 can be substituted into Eq. 10 for an alternate expression for the effective dwell fraction on the flight director

$$\bar{T}_{d_{e_{FD}}} = \bar{T}_{d_{FD}} + 0.4\,\Omega_{FD} \tag{10a}$$

Since $\bar{T}_{d_{FD}} < \bar{T}_{s_{FD}}$ and $0 \le \Omega_{FD} \le 1$, Eqs. 10 and 10a show that upper and lower bounds upon $\bar{T}_{d_{e_{FD}}}$ are respectively $\bar{T}_{s_{FD}}$ and $\bar{T}_{d_{FD}}$. Furthermore, the difference between the two bounds is only the 0.4 sec average monitoring dwell interval. This latter fact is evident from Eq. 9.

$\bar{T}_{d_{e_{FD}}}$ and $\eta_{e_{FD}}$ are theoretical constructs and are not directly observable. However, $\bar{T}_{s_{FD}}$ and $\bar{T}_{d_{FD}}$ are observable. Experimental values for $\bar{T}_{d_{FD}}$ reported in Ref. 1 are approximately 2.0 sec. $\bar{T}_{d_{FD}}$ and $\bar{T}_{s_{FD}}$ (which are the lower and upper bounds, respectively, on $\bar{T}_{d_{e_{FD}}}$) are both weak functions of the parafoveal-to-foveal gain ratio, Ω_{FD}, for constant effective dwell interval because the average monitoring dwell interval, 0.4 sec, is much less than $\bar{T}_{d_{FD}} \approx 2.0$ sec. Consequently, Ω_{FD} can be treated as an arbitrary constant in this simplified method. This is a useful property of Eq. 10 which makes it possible to establish reasonable bounds on $\bar{T}_{s_{FD}}$. (Recall that $\bar{T}_{s_{FD}}$ is equal to the reciprocal of $\bar{f}_{s_{FD}}$ determined in Eq. 4 as a function of the threshold-to-standard deviation ratio, K, in Eq. 1 and the error rate-to-displacement variance ratio $(\sigma_{\dot{x}}/\sigma_x)_f$, ie8.) $\bar{T}_{s_{FD}}$ will, in effect, be bounded from above by the largest value of K in Eq. 1 which is acceptable to the pilot, because increasing values of K represent decreasing levels of the pilot's confidence in his situation. $\bar{T}_{s_{FD}}$ will be bounded from

P-134

below by $\overline{T}_{d_{eFD}}$. In effect, $\overline{T}_{d_{eFD}}$ represents a lower bound on error rate and displacement coherencies.

The precision of this simple direct procedure for partitioning scanning workload on a single primary director control display depends on the error rate and displacement coherencies. When these coherencies are fairly high, as they usually are with a properly designed flight director, the $(\sigma_{\dot{x}}/\sigma_{x})_i$, is, in Eq. 1 are virtually equal to their input-correlated values. Thus one may start the partitioning procedure with only input-correlated error rate and displacement standard deviations determined independently by system performance calculations and without regard for the pilot's scanning remnant.

We shall next turn our attention to the effects of the pilot's scanning remnant.

A CAUSE OF LOW ERROR COHERENCE

The scanning activity required for monitoring causes the pilot to inject noise into the flight director control loops. This noise is called scanning remnant. It is the chief source of noise, because, in flight director control tasks, there is no need for pilot lead equalization in following the director commands, and hence remnant attendant to pilot lead equalization is not present.

The scanning remnant power spectral density for the "switched gain" model (Refs. 5-7) appropriate for application to the flight director is defined in Ref. 8. If we use Eq. 8a for the effective interrupt fraction, $(1 - \eta_{e_{FD}})$, and assume a sampling variability ratio $(\sigma_{T_s}/\overline{T}_s)$ of 0.5, the scanning remnant power spectral density for the flight director is

$$\Phi_{nn_s}(\omega) = \frac{0.2(1 - \Omega_{FD})\sigma^2_{FD}}{\pi\left[1 + \left(\frac{\omega \overline{T}_{d_{e_{FD}}}}{2}\right)^2\right]} \quad \frac{(\text{units})^2}{(\text{rad/sec})} \qquad (11)^*$$

* $\Phi_{nn_s}(\omega)$ is defined such that $\sigma^2_{n_s} = \int_0^\infty \Phi_{nn_s}(\omega)\,d\omega$

where $\overline{T}_{d_{eFD}}$ is given by Eq. 10 in terms of $\overline{T}_{s_{FD}}$ and Ω_{FD}. It is clear from Eqs. 9 and 10 that $\overline{T}_{d_{FD}} \leq \overline{T}_{d_{eFD}} \leq \overline{T}_{s_{FD}}$. In applying Eq. 11 to predicting the effects of scanning on system tracking error, we find it convenient to use $\overline{T}_{d_{FD}}$, the lower bound on $\overline{T}_{d_{eFD}}$, because this places an upper bound on the half-power frequency of the scanning noise and helps to make the error coherence predictions conservative. Experimental values for $\overline{T}_{d_{FD}}$ reported in Ref. 1 are approximately 2.0 sec. This places the half-power frequency, $2/\overline{T}_{d_{eFD}}$, at or below 1.0 rad/sec. In order to complete the connection between the scanning remnant power spectral density (Eq. 11) and the average monitoring scanning frequency (Eq. 1), it is necessary to digress to compute the total displayed error variance vector. In this case, "error" refers to the deviations of the displayed variables with respect to their trimmed values.

ESTIMATION OF ERROR COHERENCE AND VARIANCE

The total error variance vector, $\{\overline{\epsilon^2}\}$, is related to the coherent error variance vector, $\{\overline{\epsilon_i^2}\}$, by the equation

$$[\Delta_s]\{\overline{\epsilon^2}\} = \{\overline{\epsilon_i^2}\} \qquad (12)$$

where $[\Delta_s]$ is a square coherence matrix containing elements

$$\Delta_{s_{\epsilon_i\epsilon_j}} = \delta_{ij} - \frac{0.2(1 - \Omega_{FD})}{\pi} \int_0^\infty \left|\frac{\epsilon_i(j\omega)}{n_{\epsilon_j}(j\omega)}\right|^2 \frac{d\omega}{\left[1 + \left(\frac{\omega \overline{T}_{d_{e_i}}}{2}\right)^2\right]} \qquad (13)$$

with i components in the variance vector and j displayed axes in the flight director; and $\delta_{ij} = \begin{cases} 1; & i = j \\ 0; & i \neq j \end{cases}$ is the Kronecker delta, $\epsilon_i(j\omega)$ is the Fourier transform of the i^{th} displayed error in response to $n_{\epsilon_j}(j\omega)$, the Fourier transform of the pilot's remnant injected at the j^{th} axis of the flight director. The determinant of $[\Delta_s]$ is called the characteristic determinant of stability in the mean-square sense, or the coherence determinant. Each component of the coherent error variance vector has the form

$$\overline{\epsilon_{t_i}^2} = \sum_{\kappa=1}^{N} \int_0^\infty \left| \frac{e_i(j\omega)}{t(j\omega)} \right|_\kappa^2 \Phi_{t_\kappa}(\omega)\, d\omega \qquad (14)$$

where, for example, $t_\kappa = d_c, u_g, w_g$, the independent longitudinal inputs and disturbances: glide slope beam noise, and longitudinal and normal gust velocities; and N = 3. Thus, the vector $[\overline{\epsilon^2}]$ will, in general, be a column matrix of linear combinations of input-correlated mean-squared errors. The formal result for the total variance vector is:

$$[\overline{\epsilon^2}] = \frac{\text{adj}\,[\Delta_s]}{|\Delta_s|}\,[\overline{\epsilon_t^2}] \qquad (15)$$

The coherence determinant, $|\Delta_s|$, governs multiloop stability in the mean-square sense; therefore, it must be greater than zero. A value for the determinant which is much less than unity means that incoherent error power due to scanning remnant will be much greater than the coherent error power due to inputs and disturbances. As the coherence determinant approaches unity (its upper bound), the error power will become increasingly coherent. One of the purposes of an integrated flight director is, of course, to make the coherence determinant approach unity.

The coherence determinant depends on the display scanning statistics as well as the closed-loop frequency responses to scanning remnant. Therefore, it is desirable to obtain the coherence determinant in analytic form first, so that the average scanning statistics can be estimated in conjunction with their influence on the partition of scanning workload and mean-squared errors.

Some savings in labor will result because preliminary coherence tests on $[\Delta_s]$ (to ascertain whether or not it is greater than 0.4, for example) need be based on only the principal diagonal elements of $[\Delta_s]$. For a flight director, $[\Delta_s]$ is an upper triangular matrix; thus, the value of its determinant is equal to the product of its principal diagonal elements. The non-zero off-diagonal elements are, of course, required to verify the partition of scanning workload and to verify that approach performance requirements are satisfied.

MODIFICATION OF THE INPUT-CORRELATED PREDICTIONS OF AVERAGE THRESHOLD EXCEEDENCE FREQUENCY

The standard deviation, σ_{x_i}, of the signal, x, on display i will consist of one component, $\sigma_{o_{x_i}}$, which arises from the physical inputs and disturbances forcing the pilot-vehicle system, and a second component, $\sigma_{i_{x_i}}$, which arises from the pilot's scanning remnant. Then $\sigma_{x_i}^2 = \sigma_{o_{x_i}}^2 + \sigma_{i_{x_i}}^2$. The $\sigma_{i_{x_i}}$ component will scale linearly with the level of the injected remnant.

Exceedences of a certain absolute signal level, $|x_i| = \sqrt{K^2(\sigma_{o_{x_i}}^2 + \sigma_{i_{x_i}}^2)}$, will occur at an average frequency:

$$\overline{f}_{|x_i|} = \frac{1}{\pi} \frac{\sigma_{o_{\dot{x}_i}} \sqrt{1 + (\sigma_{i_{\dot{x}_i}} / \sigma_{o_{\dot{x}_i}})^2}}{\sigma_{o_{x_i}} \sqrt{1 + (\sigma_{i_{x_i}} / \sigma_{o_{x_i}})^2}}\, e^{-(K^2/2)} \qquad (16)$$

If we assume that the absolute level, $|x_i| = \sqrt{K^2(\sigma_{o_{x_i}}^2 + \sigma_{i_{x_i}}^2)}$, defines the pilot's threshold of indifference to the status variable x_i, i.e., the minimum change in the signal which is significant to the pilot, then we are justified in equating $\overline{f}_{s_i} = \overline{f}_{|x_i|}$ in Eq. 16, as before in the case of Eq. 1. Here, $\overline{f}_{s_i}$ is the average scanning frequency for the i^{th} secondary display. The experimental results in Ref. 1 indicate that $1.4 \leq K \leq 3.0$.

Presumably, the pilot's threshold of indifference will bear some consistent relationship (e.g., $|x_i| = 2\sigma$) to criteria for the acceptability of task errors and attitude, heading, and sideslip excursions in each portion of the flight profile. If all other contributions to the average threshold exceedence frequency are invariant, the pilot's average monitoring scanning frequency must increase to provide a lower value of the threshold-to-rms ratio, K. Therefore, his monitoring scanning workload, that is, monitoring dwell

Eq. (4) $\bar{f}_{s_{FD}} = \sum_{KES} \bar{f}_{s_K}$ where S is the set of status displays

Eq. (10) $\bar{T}_{s_{FD}} - \bar{T}_{d_K}(1-\Omega_{FD}) = \bar{T}_{de_{FD}}$ where $\bar{T}_{d_K} = 0.4$ sec
KES

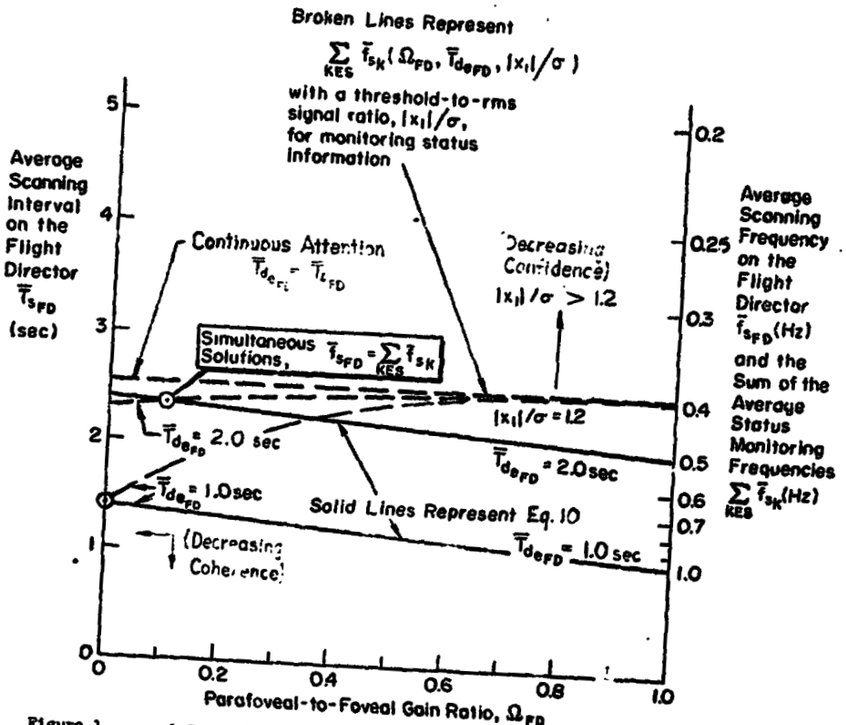

Figure 1. A Graph Illustrating the Simultaneous Solution of Two Equations for the Partition of Scanning Workload on an Integrated All-Axis Flight Director

P-134

fraction must actually increase at the expense of the flight director dwell fraction to provide a lower value of K. If the flight director dwell fraction must be so compromised that the pilot's scanning remnant causes low error coherence, task performance may be compromised, and the pilot's subjective impression of overall task workload will be high.

Conversely, if the flight director demands too much of the scanning workload, that is, too large a dwell fraction for control, because its sensitivity is too low or because the external disturbances are broadband, the pilot may have to compromise his monitoring dwell fraction to the point where K is so large that he has little confidence in the acceptability of the situation and in the satisfaction of task performance criteria. Again his subjective impression of task workload will be high. Evidently, the pilot then attempts to partition his scanning workload so that $1.4 \leq K \leq 3.0$ for reasonable confidence in the situation with acceptable error coherence, $|\Delta_s| \geq 0.4$.

Assumed values for K and $\bar{T}_{de_{FD}}$ are necessary to determine each f_{s_i} as a function of Ω_{FD} using Eq. 16 and the equality $\bar{f}_{s_i} = \bar{f}|_{x_i}|$, $i \in S$. The required $(\sigma^2_{o_{x_i}} + \sigma^2_{i_{x_i}})$ are the components of the total variance vector, $\{\epsilon^2\}$, given by Eq. 15, in which only the $\sigma^2_{i_{x_i}}$ depend on Ω_{FD} and $\bar{T}_{de_{FD}}$. The required $(\sigma^2_{o_{\dot{x}_i}} + \sigma^2_{i_{\dot{x}_i}})$ are the components of the total rate variance vector, which can be derived in a manner completely analogous to that described for the total variance vector by defining a rate coherence determinant. Again only the $\sigma^2_{i_{\dot{x}_i}}$ depend on Ω_{FD} and $\bar{T}_{de_{FD}}$. The partition of scanning workload is completed after the set of secondary $\bar{f}_{s_i}$ is summed, and Eq. 4 is satisfied. A direct graphical procedure for satisfying Eq. 4 is recommended in Ref. 1 (reproduced here in Fig. 1) using Ω_{FD} as the abscissa, $\bar{T}_{s_{FD}}$ as the ordinate, and $\bar{T}_{de_{FD}}$ as a third variable parameter. Equation 10 provides a conveniently explicit form for verifying the simultaneous satisfaction of Eq. 4 in terms of $\bar{T}_{s_{FD}}$ (or $1/\bar{f}_{s_{FD}}$), Ω_{FD} and $\bar{T}_{e_{FD}}$.

When the error coherence is fairly high, as usually is with a properly designed flight director, the ratios $(\sigma_{i_{\dot{x}_i}}/\sigma_{o_{\dot{x}_i}})^2$ and $(\sigma_{i_{x_i}}/\sigma_{o_{x_i}})^2$ in Eq. 16 are much less than unity. Hence, the secondary $\bar{f}_{s_i}$ depend primarily on the coherent error rate and displacement variances, and only weakly on the parafoveal-to-foveal gain ratio, Ω_{FD}. (Recall that $\bar{T}_{de_{FD}}$ is already closely bounded, i.e., $\bar{T}_{d_{FD}} \leq \bar{T}_{de_{FD}} \leq \bar{T}_{s_{FD}}$, where both bounds, $\bar{T}_{d_{FD}}$ and $\bar{T}_{s_{FD}}$, are also weak functions of Ω_{FD} in Eq. 10 as discussed previously.) As a consequence, the partition of scanning workload by simultaneous solution of Eqs. 4, 10, and 16 with the secondary $\bar{f}_{s_i} = \bar{f}|_{x_i}|$ can usually be simplified and approximated by ignoring the explicit dependence of the solution on Ω_{FD}, as long as the error and error rate coherencies are sufficiently high. In this case Ω_{FD} becomes an arbitrary constant. When this simplification is possible, Eq. 16 can be replaced by the form of Eq. 1 in which $(\sigma_{\dot{x}}/\sigma_x)_i \cong (\sigma_{o_{\dot{x}}}/\sigma_{o_x})_i$, the ratio of input-correlated standard deviations, and $\bar{T}_{s_{FD}}$ and $\bar{T}_{de_{FD}}$ will covary only with K as described previously in the simple direct procedure.

SUMMARY OF THE SIMPLIFIED DIRECT PROCEDURE FOR PARTITIONING SCANNING WORKLOAD ON A FLIGHT DIRECTOR

The procedure for partitioning scanning workload using Eqs. 1, 4, and 10 will be accurate provided the error displacement and error rate coherencies are reasonably high. Although the value of K, the ratio of the exceedence threshold, $|x_i|$, to σ_{x_i} ($i \in S$), may be slightly different for each secondary displayed variable x_i, the restricted bounds on K inferred from Ref. 1 suggest that a common value of K may be adequate for use in this simplified partitioning procedure.

When Eq. 1 is used for each $\bar{f}_{s_i}$ ($i \in S$) in the summation in Eq. 4, a common value of K makes it possible to write Eq. 4 as

$$\bar{f}_{s_{FD}} = \frac{e}{\pi} e^{-\frac{K^2}{2}} \sum_{i \in S} \left(\frac{\sigma_{\dot{x}_o}}{\sigma_{x_o}} \right)_i \qquad (17)$$

P-134

Since $\bar{T}_{s_{FD}} = 1/\bar{f}_{s_{FD}}$, Eq. 17 can be substituted in Eq. 10 to express

$$\bar{T}_{d_{e_{FD}}} \approx \frac{\frac{K^2}{2}}{\sum_{i \in S} \left(\frac{\sigma_{\dot{x}_o}}{\sigma_{x_o}} \right)_i} - 0.4(1 - \Omega_{FD}) \qquad (18)$$

where Ω_{FD} is treated as an arbitrary constant

K is the common ratio of each exceedence threshold $|x_i|_j$ to σ_{x_i}, $i \in S$

$\sigma_{x_{o_i}}$ is the coherent* standard deviation of the monitored variable x_i, $i \in S$

$\sigma_{\dot{x}_{o_i}}$ is the coherent* standard deviation of the time rate of change of the monitored variable x_i, $i \in S$

Equation 17 demonstrates that $\bar{f}_{s_{FD}}$ will, in effect, be bounded from below by the largest value of K which is acceptable to the pilot. (In reciprocal terms, $\bar{T}_{s_{FD}}$ will be likewise bounded from above.) Increasing values of K represent decreasing levels of the pilot's confidence in his situation. We have determined that $1.4 \leq K \leq 3.0$ for the data in Ref. 1 with a value of $K = 2.0$ being representative overall.

$\bar{T}_{s_{FD}}$ will be bounded from below by $\bar{T}_{d_{e_{FD}}}$ in Eq. 18. In effect $\bar{T}_{d_{e_{FD}}}$ represents a lower bound on error coherence and is itself bounded from below by $\bar{T}_{d_{FD}}$, which is given in terms of $\bar{T}_{s_{FD}}$ by Eq. 9 as

$$\bar{T}_{d_{FD}} = \bar{T}_{s_{FD}} - 0.4$$

where 0.4 sec is the average dwell interval for monitoring. Experimental values for $\bar{T}_{d_{FD}}$ reported in Ref. 1 are approximately 2.0 sec.

*i.e., input-correlated

A method of testing for multiloop error coherence based on Ref. 9 has been presented in order to show how to correct the partition of scanning workload in case of low error coherence caused by the pilot's injection of scanning remnant into the control loops. The method is illustrated with numerical examples and extended to the case involving two primary director control displays in Ref. 9.

REFERENCES

1. Weir, D. H., and R. H. Klein, The Measurement and Analysis of Pilot Scanning and Control Behavior During Simulated Instrument Approaches, NASA CR-1535, June 1970.

2. Hofmann, L. G., W. F. Clement, and R. E. Blodgett, A New Link Value Estimator for Scanning Workload, presented at the Ninth Annual Conference on Manual Control, MIT, 23-25 May 1973.

3. McRuer, D. T., H. R. Jex, W. F. Clement, and D. Graham, A Systems Analysis Theory for Displays in Manual Control, Systems Technology, Inc., Tech. Rept. No. 163-1, Oct. 1967 (Rev. June 1968).

4. Rice, S. O., "Mathematical Analysis of Random Noise" in N. Wax (ed.), Selected Papers on Noise and Stochastic Process, Dover Publications, New York, 1954.

5. Levison, W. H., and J. I. Elkind, Studies of Multivariable Manual Control Systems: Two-Axis Compensatory Systems with Separated Displays and Controls, NASA CR-875, Oct. 1967.

6. Allen, R. W., W. F. Clement, and H. R. Jex, Research on Display Scanning, Sampling, and Reconstruction Using Separate Main and Secondary Tracking Tasks, NASA CR-1569, July 1970.

7. Levison, W. H., and J. I. Elkind, Studies of Multivariable Manual Control Systems. Four-Axis Compensatory Systems with Separated Displays and Controls. Bolt Beranek and Newman, Inc., Rept. No. 1695, 14 Mar. 1969.

8. Clement, W. F., Random Sampling Remnant Theory Applied to Manual Control, Systems Technology, Inc., Tech. Memo No. 183-A, Mar. 1969.

9. Clement, W. F., L. G. Hofmann, and R. E. Blodgett, Application of Manual Control Display Theory to the Development of Flight Director Systems for STOL Aircraft, Part II. Multi-Axis Sampling, Pilot Workload, and Display Integration, Systems Technology, Inc. Tech. Rpt. No. 1011-2, May 1972.